International Journal of Heat and Mass Transfer 101 (2016) 562–569

Contents lists available at ScienceDirect

International Journal of Heat and Mass Transfer

journal homepage: www.elsevier.com/locate/ijhmt

Effect of scale on the modeling of radiation heat transfer in packed pebble beds

Hao Wu [a,b], Nan Gui [a], Xingtuan Yang [a], Jiyuan Tu [a,b], Shengyao Jiang [a,*]

[a] Institute of Nuclear and New Energy Technology, Collaborative Innovation Center of Advanced Nuclear Energy Technology, Key Laboratory of Advanced Reactor Engineering and Safety of Ministry of Education, Tsinghua University, Beijing 100084, China
[b] School of Aerospace, Mechanical & Manufacturing Engineering, RMIT University, Melbourne, VIC 3083, Australia

ARTICLE INFO

Article history:
Received 6 March 2016
Received in revised form 23 April 2016
Accepted 19 May 2016

Keywords:
Particle
Thermal radiation
Packed pebble bed
Voronoi tessellation
Short-range model
Discrete element method

ABSTRACT

Thermal radiation is important in high temperature packed pebble bed, which is still poorly understood. The present work is to analyze the effect of spatial scale in modeling thermal radiation of packed pebble beds. The long-range model (full integral scale), short-range model (partial integral scale) and microscopic models (sub-particle scale) are compared and analyzed with reference to existing correlations. In high temperature packed pebble beds, the long-range model takes into account all possible radiation between surrounding spheres, even those that are not direct Voronoi neighbors, whereas the short-range model considers only a portion nearby. It is found that when solid conductivity is much greater than the effective thermal conductivity of radiation ($k_s \gg k_r$ or $\Lambda > 10$), the long-range model provides better results than the short-range model in predicting the radiative heat exchange. The short-range model overestimates solid conductivity at low temperatures (lower than 1215 °C) when $k_s \sim O(k_r)$ (or $\Lambda < 10$) while underestimating radiative heat exchange. It therefore still provides predictions for total heat exchange that is in good agreement with experimental data in cases where the errors cancel out. Moreover, the short-range radiation model is more computationally efficient than the long-range model and microscopic model to compute view factor between particles of Voronoi neighbors.

1. Introduction

High temperature gas-cooled reactor (HTGR) is a promising type of generation IV nuclear reactor with its inherent safety, high efficiency and potential usage for hydrogen production [1]. The reactor core of HTGR is a packed pebble bed composed of large quantities of randomly packed mono-sized spherical particles. The packed pebble bed operates at about 800 °C under normal conditions [2]. Local temperature of the packed pebble bed can reach 1600 °C under accidental conditions. Thus, radiation is an important issue of thermal heat transfer for HTGR.

Many researches have been performed to improve the heat transfer study of packed pebble bed. For example, for experimental investigations, SANA-I is a classic experiment of packed pebble bed, which is filled with about 9500 graphite particles of 60 mm in diameter and heated by electrical resistance heating elements [3]. The bed is operated in inert gas (helium or nitrogen) atmosphere and the effect of natural convection cannot be neglected under lower heating power. The HTTU test is another new experiment with negligible natural convection [4]. The facility is filled with nitrogen as interstitial gas and operated under very low pressures. There are about 25,000 machined graphite spheres of 60 mm in diameter. The annular core of the bed is 0.6 m and 2.3 m in inner and outer diameters respectively, and 1.2 m in height.

Moreover, for theoretical and numerical study, the macroscopic models based on the porous-medium assumption of the packed pebble bed have been widely used in the simulation [5] and analysis of transient thermal hydraulics of HTGR [6]. Basically, there are three types of heat transfer modes in the packed pebble beds, i.e. the convective, conduction and thermal radiation heat transfer. For example, based on dimensional analysis of the convective heat transfer, the Rayleigh–Darcy number for natural convection will increase greatly at lower temperature and the contribution of natural convection to total heat transport will increase consequentially [7]. For other kinds of heat transfer modes, the concept of effective thermal conductivity of the packed pebble bed (k_{eff}) is always incorporated to simplify the handling of heat transfer. It is a critical parameter for HTGR and includes the fluid-particle conduction, particle–particle heat conduction, and particle–particle thermal radiation. k_{eff} is usually obtained from experimental data. It can affect the maximum temperature in nuclear fuel and vessel under especially limiting events, which is closely related to the

* Corresponding author.
E-mail addresses: guinan@mail.tsinghua.edu.cn (N. Gui), shengyaojiang@sina.com (S.Y. Jiang).

http://dx.doi.org/10.1016/j.ijheatmasstransfer.2016.05.090
0017-9310/

nuclear safety margin of HTGR [3]. To date, theoretical models of heat conduction in packed pebble beds of rough and mono-sized spheres have been well developed and verified by experiments [8,9]. However, the particle–particle thermal radiation models are still poorly developed. The existing models and empirical correlations usually deviate from each other largely [10].

As temperature rises, the amount of heat conduction almost remains a constant. Nevertheless, the amount of thermal radiation heat exchange between particles will increase rapidly and dominate the process of heat transfer in high temperature packed pebble bed [11]. Comparing to conduction between particles at contact, thermal radiation is much more complicated for numerical computation because of its non-contact and long-range interactions. As well known, the discrete element method (DEM), can be used to simulate the motion of all particles in the particle system [12] and the packing state of particle beds [13], and explore the distinctive features of packing structures [14]. With the aid of space discretization realized by Voronoi tessellation [15], it is also possible to be used for analyzing the heat transfer mechanisms [16–18] of mono or multi-sized particles based on the. Thus, with some extensions if necessary, it is a good approach to fulfill the purpose of radiative heat transfer modeling of the packed pebble bed.

Therefore, to improve the modeling of radiative heat transfer, in this work, the thermal radiation heat exchanges are computed by three models respectively to analyze the effect of spatial scales based on the DEM data of particle packing. The scales include the full integral scale of thermal radiation, the partial integral scale, and the sub-particle scale. In the sub-particle scale, the non-uniform temperature distribution over the particle surface is considered. In addition, the existing correlations obtained from experimental data statistically are used here for referential comparison.

2. Numerical model

In the Lagrangian approach, thermal radiation between particles is considered individually. It is assumed that every particle in the packed pebble bed is an isothermal body and the solid conductivity within the particle is infinity. When one particle only exchanges radiation heat with the nearby neighbors and neglects the radiative heat transfer with far particles, it is so-called the short-range radiation model. On the contrary, it is extended to the long-range radiation model when all the peripheral particles are taken into account for radiative heat exchanges.

2.1. Short-range radiation model

2.1.1. Model formulations

When the particle flow in the bed is quite dense and slow or even quasi-static (e.g. the packed pebble bed in HTGR), the porosity is about 0.4 in stagnant state. It is reasonable to assume that only neighboring particles, which may be technically separated by Voronoi tessellations [15], can exchange radiative energies. Voronoi tessellation is a numerical method to discretize the spatial domain into a group of independent Voronoi cells with only one particle staying inside each cell, e.g. the discretization of the packed pebble bed of SANA-I (Fig. 1a). The bed in Fig. 1a is 1.0 m in height, and 6.5 cm and 750 cm in inner and outer radii, respectively. Every cell is a polyhedron and an interface exists between each pair of neighboring particles (Fig. 1b). To ensure energy conservation, it is assumed that all the radiative heat passed through the interface of polyhedrons is obtained by the neighboring particle. Hence, the view factor from one sphere to its neighboring particle is equivalent to the interface of Voronoi tessellations.

Then, the view factor from one sphere to its enclosing polygon (Fig. 2a) can be decomposed into the sphere to some right-angled

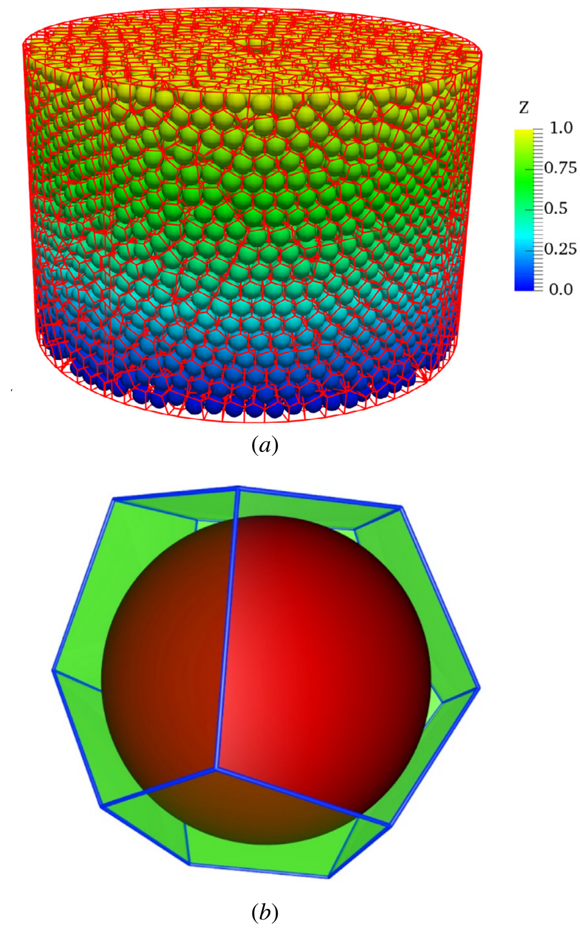

Fig. 1. Voronoi tessellation of SANA-I (a) and a single Voronoi element (b) (particle ID = 2562, Z is particle center height).

triangles (Fig. 2b, where point A is the projection of the sphere center O onto the interface and line AB is perpendicular to line BC). The analytical solution of the view factor [19] is

$$V = \frac{1}{4\pi}\arccos\left(\frac{1}{B_3}\right) - \frac{1}{8\pi}\arcsin\left[\frac{(1-B_1^2)B_3^2-2}{(1+B_1^2)B_3^2}\right] - \frac{1}{16} \quad (1)$$

where $B_1 = Y/H$, $B_3 = L/Y$.

The radiant heat flux $Q^r_{i,j}$ between a pair of Voronoi neighboring spheres (particle i and particle j) can be simplified as:

$$Q^r_{i,j} = \frac{\sigma\left(T_i^4 - T_j^4\right)}{\frac{1-\varepsilon}{\varepsilon A_i} + \frac{1}{A_i V_{i,j}} + \frac{1-\varepsilon}{\varepsilon A_j}} \quad (2)$$

where σ is Stephan–Boltzmann constant, A_i, A_j and T_i, T_j are the surface area and temperature in Kelvin of particle i and particle j respectively. ε and $V_{i,j}$ are surface emissivity and view factor between the pair of particles. In present model, only the thermal radiation heat transfer is considered. Then, the steady thermal equilibrium equation of particle i is

$$\sum_{j=1}^{n} Q^r_{i,j} = 0 \quad (3)$$

where n is the number of Voronoi neighboring particles of particle i. When Eq. (3) is applied to every particle, a solvable group of linear equations can be obtained with additional thermal boundary conditions.

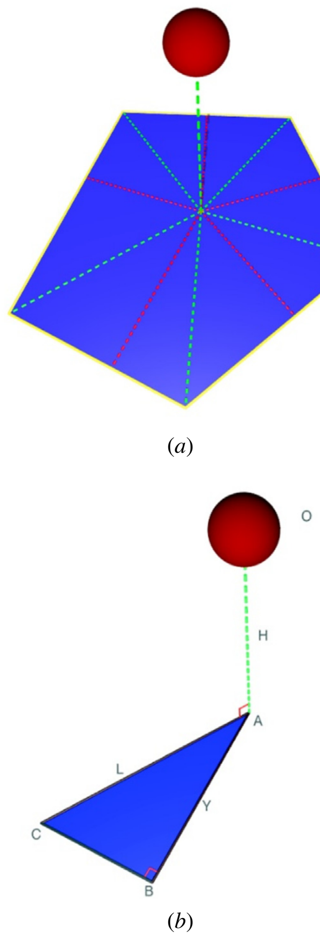

Fig. 2. View factor from a sphere to polygon (a) and its decomposition (b).

After solving Eq. (3), the temperature of every particle can be obtained. Then, they can be used for computation of some important variables of the bed, such as the effective thermal conductivity and radiation exchange factor. These variables are used to evaluate the accuracy of the model prediction by comparison with existing correlations and experimental data.

2.1.2. Variables for comparison

From the viewpoint of engineering, two important variables are used here for comparison and analysis. The first one is the effective thermal conductivity of radiation. For the cylindrical packed pebble bed, it is defined as follows:

$$k_r = \frac{Q_r}{2\pi H \Delta T} \ln(r_2/r_1) \tag{4}$$

where Q_r, H and ΔT are the heating power of the inner wall, the height of packed pebble bed and the temperature difference between the hot and cold walls, respectively. r_1 and r_2 are the inner and outer radii of the bed, respectively.

The second important variable is the dimensionless radiation exchange factor F, which is defined as

$$F = \frac{k_r}{4\sigma d_p T_m^3} \tag{5}$$

where d_p and T_{m} are particle diameter and arithmetic average of all particle temperature of the bed respectively.

2.1.3. Existing correlations

To obtain k_r and F in engineering, some correlations of them are available for estimating the thermal radiation of the packed pebble bed, e.g. the Schotte correlation, Kunii–Smith correlation, and Zehner–Bauer–Schlünder (ZBS) correlation.

The porosity, surface emissivity and solid conductivity are incorporated in the Schotte correlation [20] which is formulated as:

$$k_r = \frac{1-\varphi}{1/k_s + 1/k_r^0} + \varphi k_r^0 \tag{6}$$

$$k_r^0 = 4\varepsilon d_p \sigma T^3 \tag{7}$$

where φ is the porosity of the bed and k_s is the solid conductivity.

In the Kunii–Smith correlation, the effective thermal conductivity k_{eff} (including conduction and radiation) is formulated as

$$\frac{k_{eff}}{k_f} = \varphi\left(1 + \frac{\beta k_{rv}}{k_f}\right) + \frac{\beta(1-\varphi)}{\left(\psi_t + k_{rs}/k_f\right)^{-1} + \gamma k_f/k_s} \tag{8}$$

$$k_{rv} = \frac{4 d_p \sigma T^3}{1 + \frac{\varphi}{2(1-\varphi)}\frac{1-\varepsilon}{\varepsilon}} \tag{9}$$

$$k_{rs} = 4 d_p \sigma T^3 \frac{\varepsilon}{1-\varepsilon} \tag{10}$$

where β, ψ_t and γ are geometry parameters. k_f is the conductivity of fluid. When k_{rv} and k_{rs} are close to 0, k_{eff} will be the effective thermal conductivity for heat conduction (k_c). Thus, the effective thermal conductivity for thermal radiation is $k_r = k_{eff} - k_c$.

In the ZBS correlation, the radiation exchange factor F is expressed as

$$F = \left[1 - \sqrt{1-\varphi}\right]\varphi + \frac{\sqrt{1-\varphi}}{2/\varepsilon - 1} \cdot \frac{B+1}{B} \cdot \frac{1}{1 + 1/[(2/\varepsilon - 1)\Lambda]} \tag{11}$$

where $\Lambda = k_s/(4 d_p \sigma T^3)$ and $B = 1.25[(1-\varphi)/\varphi]^{10/9}$. The ZBS correlation has been applied in thermal hydraulic analysis of packed pebble bed experiments and HTGR [3,6]. It was found that the Kunii–Smith correlation and Zehner–Bauer–Schlünder (ZBS) correlation are in good agreement with experimental data at high temperature [21]. Thus, these models are used here as referential data for comparison.

2.1.4. Comparisons

In Fig. 3a, numerical results of the effective thermal conductivity of radiation (k_r) obtained by the short-range model are compared to the existing correlations. The surface emissivity of graphite pebbles is 0.8. It is shown that k_r of the short-range model is much less than the existing correlations at high temperature. Moreover, the predicted values of radiation exchange factor F (Fig. 3b) also deviate greatly from the aforementioned correlations at high surface emissivity ($\varepsilon > 0.6$).

Thus, the short-range model is not suitable for predicting the high-temperature particle radiation, because it underestimates the effective thermal conductivity and radiation exchange factor at high temperature and high surface emissivity. In other words, the long-range radiation model should be considered to correct the underestimation.

2.2. Long-range radiation

In the long-range radiation model, it is of vital importance to calculate the view factors between any two spheres and from sphere to wall to study the thermal radiation of packed pebble bed. Some analytical solutions of view factor between primitives

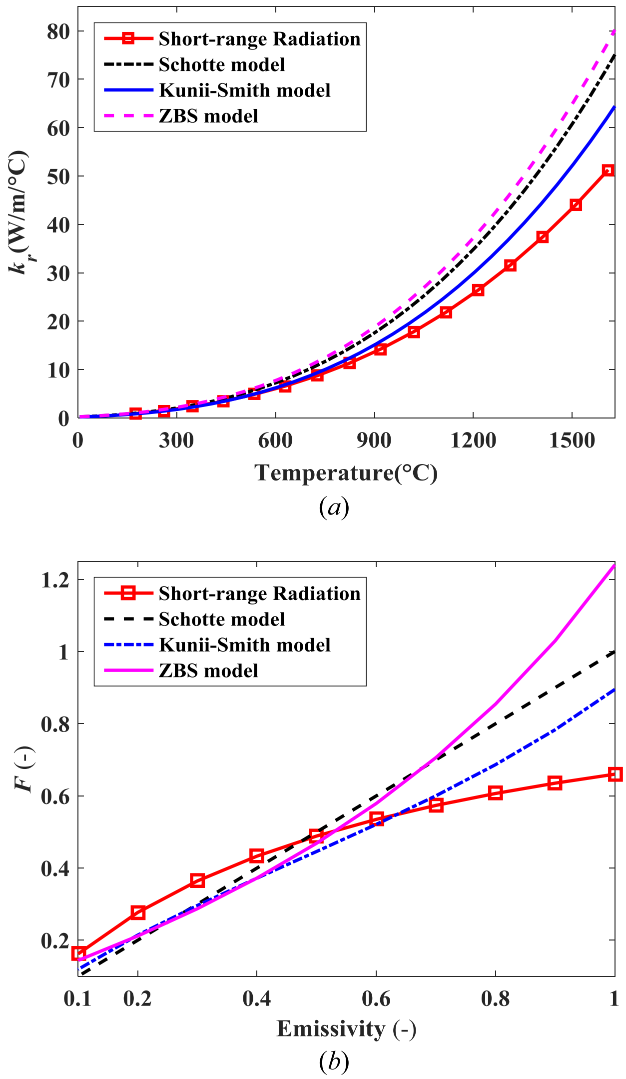

Fig. 3. Effective thermal conductivity (a) and radiation exchange factor (b) for short-range radiation model (solid conductivity is infinity).

such as sphere, plane and cylinder are available [22]. The analytical expression of view factor between two unit spheres without any blockage can be obtained by the general solution method [23]:

$$V = \frac{1}{\pi h}\int_0^{\frac{\pi}{2}} \frac{2\eta - \sin(2\eta)}{\sqrt{h^2 - 4\cos^2(\eta)}}\sin(2\eta)d\eta \tag{12}$$

where h is the distance between two unit spheres and $h \geqslant 2$. For two spheres at contact ($h < 2$), the solution is deduced to

$$V = \frac{4}{\pi h(2+h)}\int_{\arccos(\frac{h^2}{4})}^{\frac{\pi}{2}} \frac{2\eta - \sin(2\eta)}{\sqrt{h^2 - 4\cos^2(\eta)}}\sin(2\eta)d\eta + \frac{h^2}{16}(h-2) \tag{13}$$

However, thermal radiation heat exchange between two spheres in packed pebble bed is blocked greatly by each other. Adaptive integration [24] and Tanaka integral [2] are traditional numerical methods to compute the view factor between two spheres or planes subject to any blockage. For complex three-dimensional geometries, it is recommended to use the Monte Carlo method (MCM) by using ray tracing [25,26] to calculate the view factor. The MCM can be accelerated by multithreading and graphics processing unit (GPU) and much faster than integral method for computation [27].

Although the view factor between particles of the packed pebble bed is getting small when inter-particle distance h increases (Fig. 4), the thermal radiation exchange still exists between long-distance spheres that are not Voronoi neighboring particles in the bed. Note that the view factor for all Voronoi neighbors under the short-range model is only accumulated to about 0.8343 (Fig. 4). However, the averagely cumulative sums of view factor for two and three peripheral layers of Voronoi neighbors are about 0.9869 and 0.9991, respectively, (e.g. three layers of particles enclosing the white particle are composed of about 200 nearby particles in Fig. 4a). Thus, it is considered that, under the long-range condition, it is almost an enclosed space for the while particle to exchange radiative heat with three peripheral layers of Voronoi neighbors. In other words, it is sufficient to compute the view factors of the white particle within the three layers of particles. It is also similar to compute the view factors for other particles.

Suppose every particle is an opaque and gray body and its surface radiosity $\boldsymbol{J}_i$ is

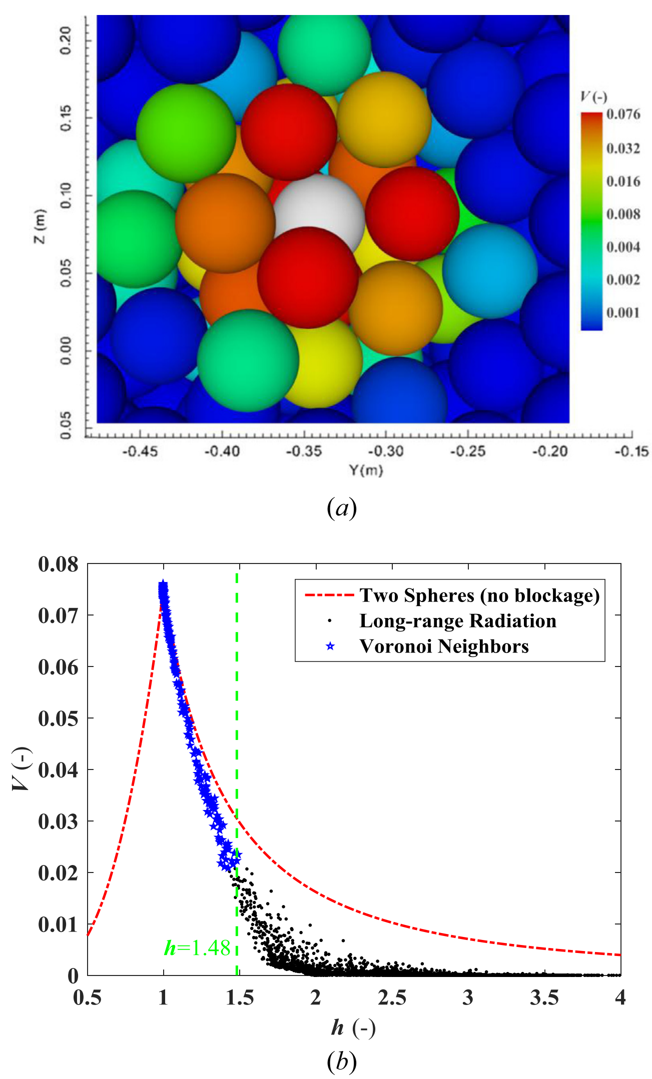

Fig. 4. Local view factor distribution in pebble bed ((a): particle ID = 5595 and colored in white, (b): view factor to distance for 20 particles, $h = r/d_p$, r is the distance between two particle center).

$$\boldsymbol{J}_i = \varepsilon\sigma T_i^4 + (1-\varepsilon)\boldsymbol{G}_i \tag{14}$$

where $\boldsymbol{G}_i$ is irradiation from all other surfaces. For the long-range model, it is

$$\boldsymbol{G}_i = \sum_{j=1}^{n} V_{i,j}\boldsymbol{J}_j \tag{15}$$

where $V_{i,j}$ is the view factor from particle i to particle j. n is the number of all particles of $V_{i,j} > 0$ for particle i. The net radiative heat flux $\boldsymbol{q}_i$ will be

$$\boldsymbol{q}_i = \boldsymbol{G}_i - \boldsymbol{J}_i \tag{16}$$

Similarly, after solving the thermal equilibrium equations of all particles, the effective thermal conductivity can be computed by the long-range radiation model, as shown in Fig. 5. For surface emissivity $\varepsilon = 0.8$, the results are in good agreement with the ZBS model at high temperature, obviously better than the short-range model. Nevertheless, the present model is in general accord with the Kunii and Smith model for $\varepsilon = 1.0$, where the ZBS model is obviously greater than the predicted value over 2000 °C.

To say conclusively, comparing Fig. 5 with Fig. 4, it is generally indicated that the long-range model is better than the short-range model for predicting the heat exchange in packed pebble beds, when solid conductivity is much greater than the effective thermal conductivity of radiation ($k_s \gg k_r$).

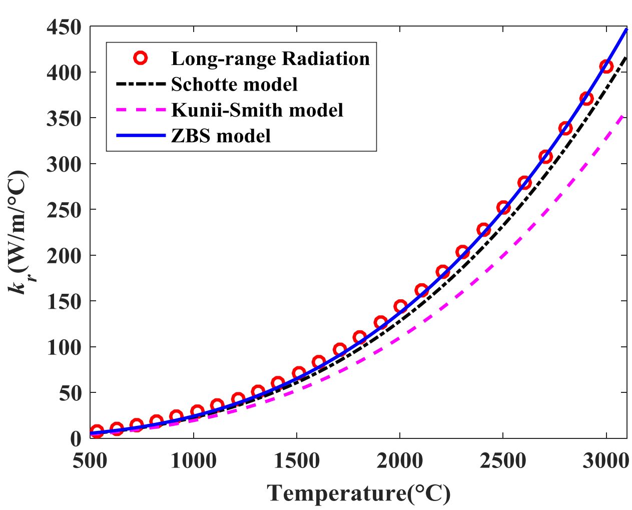

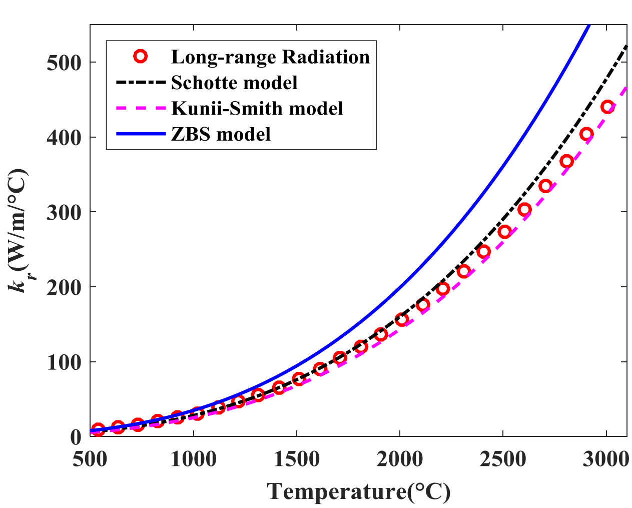

Fig. 5. Effective thermal conductivity for long-range radiation model for surface emissivity $\varepsilon = 0.8$ (a) and $\varepsilon = 1.0$ (b).

2.3. Microscopic model

As aforementioned, when $k_s \gg k_r$ or the particles are very small, the particle surface temperature is uniform and the integral scale model is strictly valid for packed pebble bed. However, for ordered packing [28], the effect of finite solid conductivity needs to be considered when $\Lambda = k_s/(4d_p\sigma T^3) < 10$. For example, Λ is 4.3 at 750 °C and may decrease to 0.5 at 1600 °C for HTGR. For that condition, the microscopic model should be used certainly to address the non-uniform sub-particle scale temperature distribution of temperature within the particle.

In the microscopic model, the particle surface is divided into a series of meshes and every mesh is considered as an isothermal surface. From the result of long-range radiation model (Fig. 6), the heating power from inner wall is 27.2 kW without conduction between particles. A particle with 2840 meshes is used to investigate the microscopic effect. Moreover, heat conduction flux inside the particle volume is much less than thermal radiation flux, e.g. accounting for only about 7% of total flux at $k_s = 50$ W/(m·°C). Hence, heat conduction inside the particle could be neglected here and the meshes inside the particle are not considered.

For simplicity, the temperature and radiosity of all other particles are kept the same. The radiative heat flux of all meshes can be computed after obtaining the view factors from them to the neighboring spheres. The heat flux of heat conduction $Q_{i,j}^m$ between two adjacent meshes is

$$Q_{i,j}^m = -Ak_s(T_i - T_j)/L \tag{17}$$

where A and L are the area of contact surface and the distance between two meshes respectively. T_i and T_j are the temperature of two meshes respectively. The steady thermal equilibrium equation for every mesh is

$$Q_i^r + \sum_{j=1}^{n} Q_{i,j}^m = 0 \tag{18}$$

where Q_i^r is radiative heat flux for mesh i. The equations for all meshes are non-linear and can be solved by iterative method.

The radial temperature gradient without heat conduction (Fig. 7a) is 101.2 °C per 60 mm, which is about twice as that in the long-range radiation model (50.9 °C per 60 mm). Thus, in microscopic model, it is necessary to improve the formulation of effective thermal conductivity of radiation $k_{r,mic}$ by

$$k_{r,mic} = k_{r,l}\frac{1}{1 + Y_m/Y_p} \tag{19}$$

where $k_{r,l}$ is the result of the long-range radiation model, Y_m and Y_p are the radial temperature gradients in the microscopic model and the long-range radiation model, respectively. $k_{r,mic}$ of different solid conductivities is shown in Fig. 7b at $k_{r,l} = 12.86$ W/(m·°C). The present microscopic method is generally in good concordance with Schotte correlation and only deviates from the Kunii–Smith correlation at $\Lambda > 1$ and from the ZBS correlation at $\Lambda < 1$. By fitting the data for surface emissivity $\varepsilon = 0.8$, the following expression is obtained:

$$k_{r,mic} = k_{r,l}\frac{1}{1 + 2/(\Lambda + 1)} \tag{20}$$

which is suggested as correction of the long-range model.

Finally, for the total effective thermal conductivity k_e of the packed pebble bed, both the radiation part k_r and the heat

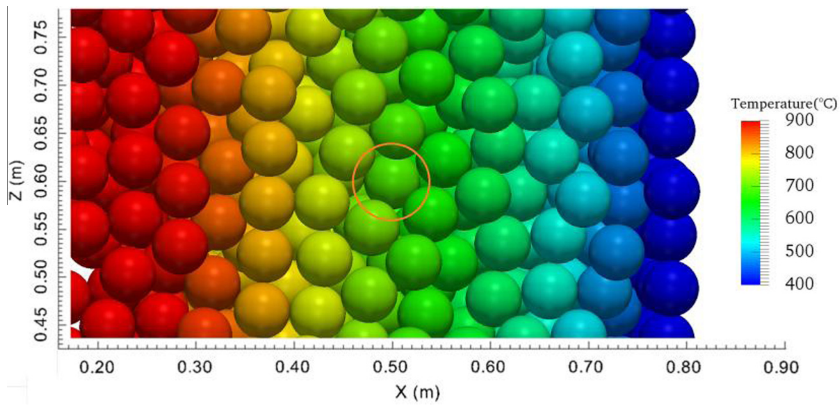

Fig. 6. Local temperature distribution in the pebble bed in long-range radiation model (ε = 0.8, the marked particle ID = 5595, temperature is 689.7 °C).

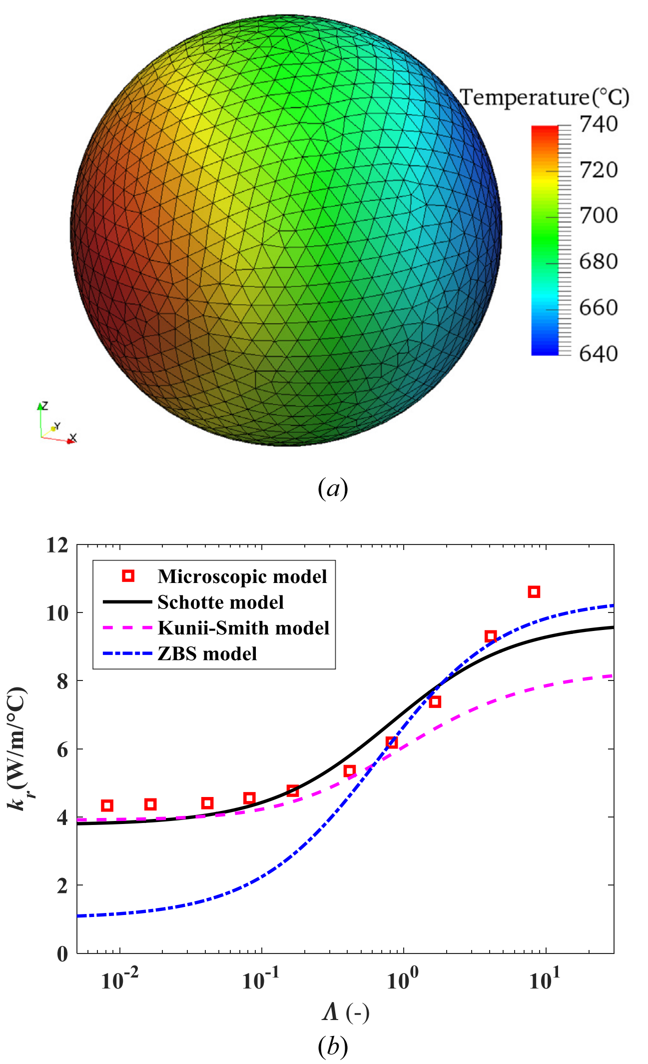

Fig. 7. Surface temperature profile of marked particle without heat conduction (a) and the effective thermal conductivity at the microscopic model (b).

conduction part k_c need to be considered, i.e. $k_e = k_r + k_c$. Notice that the heat conduction part remains almost constant at different temperatures. For example, k_c is about 5 W/(m·°C) for SANA-I, where the interstitial gas is helium. Although the total effective thermal conductivity predicted by the microscopic model is a bit lower than the SANA-I experiment which fluctuates considerably (Fig. 8), it is very close to the predictions of ZBS correlation and Antwerpen's correlation [11]. Thus, together with Fig. 7, we tend to consider that the accuracy for present microscopic model is acceptable.

2.4. Further discussion for finite thermal conductivity

2.4.1. Total effective thermal conductivity when $k_s \sim O(k_r)$

As complementary comparisons, in this section, the thermal radiations of packed pebble bed predicted by different models are compared with the experimental data of HTTU test (Fig. 9, [4]. It is seen from Fig. 9 that the microscopic model is in good agreement with experimental data and ZBS correlation. It is the most accurate model, although it is not feasible in practical computation since it is computationally unacceptable to calculate the view factors between all the meshes over the surface of all surrounding particles of the beds.

In the HTTU test, the natural convection can be neglected and the conduction part of effective thermal conductivity k_c is about 2 W/(m·°C) [4]. The dependence of conductivity of graphite material on temperature is [3]

$$k_s = 186 - 39.54 \times 10^{-2} t + 4.89 \times 10^{-4} t^2 - 2.91 \times 10^{-7} t^3 + 6.6 \times 10^{-11} t^4 \tag{21}$$

where t is the temperature in °C. Thus, the conductivity k_s is finite, and the condition $k_s \gg k_r$ is not guaranteed.

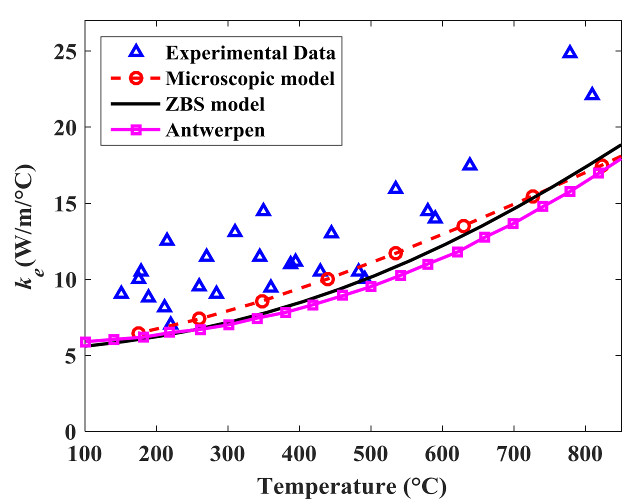

Fig. 8. Comparison between numerical model and experimental data of total effective thermal conductivity for SANA-I.

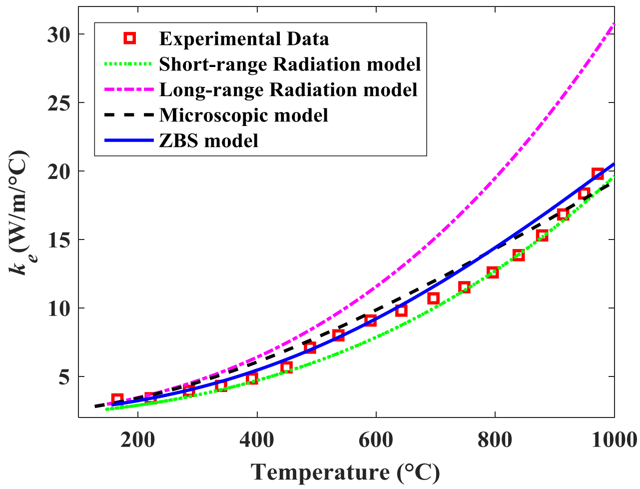

Fig. 9. Comparison between different models and experimental data of total effective thermal conductivity for HTTU.

Moreover, as indicated by Fig. 9, the total effective thermal conductivity predicted by the long-range radiation model is significantly higher than experimental data at high temperature. It is because the condition $k_s \gg k_r$ is not met at current condition. The effect of finite solid conductivity plays a key role in reducing the rate of heat exchange. Thus, although the long-range model is an accurate model in calculating the full view factors, it will still overestimate the total effective thermal conductivity of the bed under the condition of infinite thermal conductivity of particle. Thus, the long-range radiation model needs to be modified in practical applications under operation conditions when the solid conductivity k_s are in the same order of k_r.

In contrast, although with somewhat overestimation of solid thermal conductivity, the short-range model underestimates the view factor and thermal radiation for each particle. The underestimation of radiative heat transfer may, to some extent, counterbalance the overestimation of conductive heat transfer, which results in an improved prediction of the total effective thermal conductivity for the short-range model than the long-range model at $k_s \sim O(k_r)$. As indicated from Fig. 10, the prediction errors for the short-range model may cancel out under $T < 1215$ °C. Hence, if $k_s \sim O(k_r)$, the short-range model can still be applied when the operating temperature is lower than 1215 °C.

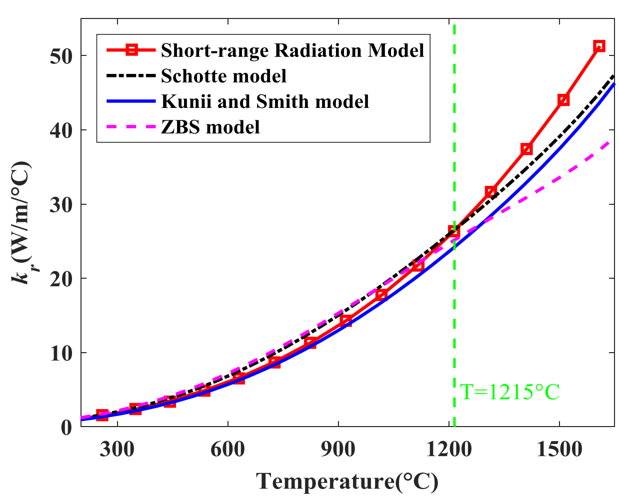

Fig. 10. Effective thermal conductivity of radiation at high temperature ranges considering solid conductivity for HTTU.

2.4.2. Feasible choice for overall bed

As aforementioned, although with the most accuracy, the microscopic model is still computationally not feasible. Then, what is the feasible choice for prediction of overall heat transfer of practical packed bed? It is suggested that the short-range radiation model could be one of such choice, especially for the packed pebble bed HTGR with graphite materials ($k_s \sim O(k_r)$) (see Fig. 10).

The heat conduction between particle i and particle j at contact is

$$Q^c_{i,j} = H(T_i - T_j) \tag{22}$$

where H is contact conductance as described in Nguyen et al. [29]. The steady heat equation for particle i combined with particle–particle radiation between Voronoi neighbors can be expressed as

$$\sum_{j=1}^{n} Q^c_{i,j} + \sum_{k=1}^{m} Q^r_{i,k} = 0 \tag{23}$$

After solving Eq. (23) for all the particles, the temperature distribution throughout the packed pebble bed can be obtained. The results obtained by the short-range radiation model for HTTU are shown in Fig. 11, which are in good agreement with

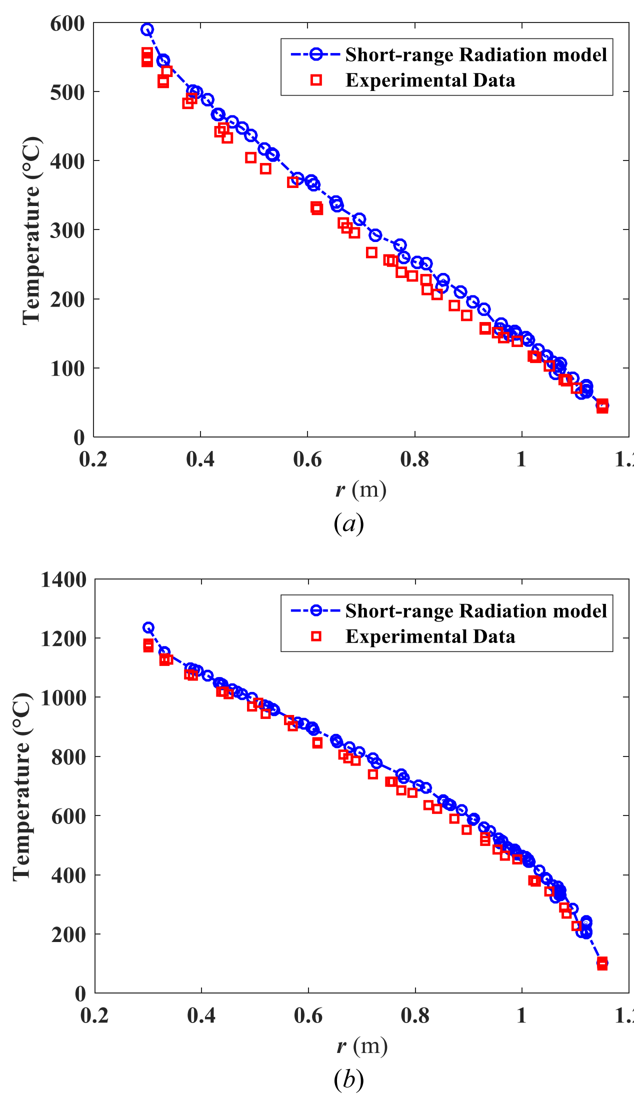

Fig. 11. Simulation results of short-range radiation model for HTTU at half height with different heating power ((a): 20 kW tests, (b): 82 kW tests).

experimental measurements under different heating powers. Thus, it is sure that the short-range model can be used for practical beds under low temperature ranges (generally not large than 1215 °C) at $k_s \sim O(k_r)$.

3. Conclusion

Thermal radiation heat exchange in three-dimensional packed pebble bed is discussed from full integral scales (long-range model) to sub-particle scales (microscopic scale model) through partial integral particle scales (short-range model). For the full and partial integral scales, all the spheres in packed pebble beds are assumed as isothermal bodies with infinite thermal conductivity, or $k_s \gg k_r$. For the sub-particle scale, the effect of finite conductivity, namely $k_s \sim O(k_r)$, is considered.

With comparison to existing data and correlations, it is found that:

(1) The long-range radiation model is an accurate approach since all surrounding spheres with possible thermal radiative heat exchange are considered. It is usually enough to consider three peripheral layers of Voronoi neighbors (about 200 particles) as its cumulative sum of view factors is 0.9991. However, the long-range model is subject to the condition of $\Lambda > 10$ or $k_s \gg k_r$.

(2) For the short-range model, it is not suitable for large conductivity materials ($k_s \gg k_r$). Alternatively, it can be used for $k_s \sim O(k_r)$ or $\Lambda < 10$. The overestimation of solid thermal conductivity and underestimation of the view factors and radiative heat transfer may lead to good predictions of the overall effective thermal conductivity in cases the errors cancel out. As a result, the accuracy of short-range radiation model is acceptable at low temperatures lower than 1215 °C. Under this condition, it is efficient to use the short-range model to compute the view factors and obtain the temperature field of the packed pebble beds with acceptable errors.

(3) Although the microscopic model is the most accurate model even for $k_s \sim O(k_r)$, it is computationally unacceptable for practical used of thermal heat transfer prediction of the overall packed pebble bed. However, it can be used for improving the prediction of short-range and long-range models. A correction of the long-range model prediction is suggested in present work.

Acknowledgements

The authors are grateful for the support of this research by the National Natural Science Foundations of China (Grant No. 51576211), the Science Fund for Creative Research Groups of National Natural Science Foundation of China (Grant No. 51321002), and the Foundation for the Author of National Excellent Doctoral Dissertation of PR China (FANEDD, Grant No. 201438). This work is also supported financially by China Scholarship Council (CSC) under the Grant No. 201506210365.

References

[1] Z. Zhang, Y. Sun, Economic potential of modular reactor nuclear power plants based on the Chinese HTR-PM project, Nucl. Eng. Des. 237 (2007) 2265–2274.
[2] Y.T. Feng, K. Han, An accurate evaluation of geometric view factors for modelling radiative heat transfer in randomly packed beds of equally sized spheres, Int. J. Heat Mass Transfer 55 (2012) 6374–6383.
[3] H. Niessen, S. Ball, Heat Transport and Afterheat Removal for Gas Cooled Reactors under Accident Conditions. IAEA-TECDOC-1163, International Atomic Energy Agency, 2000.
[4] P.G. Rousseau, C.G. du Toit, W. van Antwerpen, H.J. van Antwerpen, Separate effects tests to determine the effective thermal conductivity in the PBMR HTTU test facility, Nucl. Eng. Des. 271 (2014) 444–458.
[5] S. Becker, E. Laurien, Three-dimensional numerical simulation of flow and heat transport in high-temperature nuclear reactors, Nucl. Eng. Des. 222 (2003) 189–201.
[6] Y. Zheng, J. Lapins, E. Laurien, L. Shi, Z. Zhang, Thermal hydraulic analysis of a pebble-bed modular high temperature gas-cooled reactor with ATTICA3D and THERMIX codes, Nucl. Eng. Des. 246 (2012) 286–297.
[7] D.A. Nield, A. Bejan, Convection in Porous Media, fourth ed., Springer, New York, 2013.
[8] M. Bahrami, M.M. Yovanovich, J.R. Culham, Effective thermal conductivity of rough spherical packed beds, Int. J. Heat Mass Transfer 49 (2006) 3691–3701.
[9] G. Weidenfeld, Y. Weiss, H. Kalman, A theoretical model for effective thermal conductivity (ETC) of particulate beds under compression, Granular Matter 6 (2004) 121–129.
[10] W. van Antwerpen, C.G. du Toit, P.G. Rousseau, A review of correlations to model the packing structure and effective thermal conductivity in packed beds of mono-sized spherical particles, Nucl. Eng. Des. 240 (2010) 1803–1818.
[11] W. van Antwerpen, P.G. Rousseau, C.G. du Toit, Multi-sphere unit cell model to calculate the effective thermal conductivity in packed pebble beds of mono-sized spheres, Nucl. Eng. Des. 247 (2012) 183–201.
[12] C.H. Rycroft, Multiscale Modeling in Granular Flow, Massachusetts Institute of Technology, 2007.
[13] H. Suikkanen, J. Ritvanen, P. Jalali, R. Kyrki-Rajamäki, Discrete element modelling of pebble packing in pebble bed reactors, Nucl. Eng. Des. 273 (2014) 24–32.
[14] L.Y. Yi, K.J. Dong, R.P. Zou, A.B. Yu, Radical tessellation of the packing of ternary mixtures of spheres, Powder Technol. 224 (2012) 129–137.
[15] C.H. Rycroft, VORO++: a three-dimensional Voronoi cell library in C++, Chaos 19 (2009) 041111.
[16] P. Camps, M. Baes, W. Saftly, Using 3D Voronoi grids in radiative transfer simulations, Astron. Astrophys. 560 (2013) A35.
[17] G.J. Cheng, A.B. Yu, Particle scale evaluation of the effective thermal conductivity from the structure of a packed bed: radiation heat transfer, Ind. Eng. Chem. Res. 52 (2013) 12202–12211.
[18] G.J. Cheng, A.B. Yu, P. Zulli, Evaluation of effective thermal conductivity from the structure of a packed bed, Chem. Eng. Sci. 54 (1999) 4199–4209.
[19] A. Feingold, K.G. Gupta, New analytical approach to the evaluation of configuration factors in radiation from spheres and infinitely long cylinders, J. Heat Transfer 92 (1970) 69–76.
[20] W. Schotte, Thermal conductivity of packed beds, AIChE J. 6 (1960) 63–67.
[21] K. Nasr, R. Viskanta, S. Ramadhyani, An experimental evaluation of the effective thermal conductivities of packed beds at high temperatures, J. Heat Transfer 116 (1994) 829–837.
[22] J.R. Howell, A Catalog of Radiation Configuration Factors, McGraw-Hill, 1982.
[23] S. Tanaka, Exact view-factor analysis for radiation from a sphere to another sphere linked with a coaxial cylinder, Rev. Faculty Maritime Sci. Kobe Univ. 5 (2008) 85–92.
[24] G.N. Walton, Calculation of Obstructed View Factors by Adaptive Integration, National Institute of Standards and Technology, Gaithersburg, 2002.
[25] J.D. Maltby, P.J. Burns, Performance, accuracy, and convergence in a three-dimensional Monte Carlo radiative heat transfer simulation, Numer. Heat Transfer Part B 19 (1991) 191–209.
[26] T. Walker, S.C. Xue, G.W. Barton, Numerical determination of radiative view factors using ray tracing, J. Heat Transfer 132 (2010) 072702.
[27] T. Walker, The Use of Primitives in the Calculation of Radiative View Factors, University of Sydney, Sydney, 2014.
[28] B. Singh, M. Kaviany, Effect of solid conductivity on radiative heat transfer in packed beds, Int. J. Heat Mass Transfer 37 (1994) 2579–2583.
[29] V.D. Nguyen, C. Cogné, M. Guessasma, E. Bellenger, J. Fortin, Discrete modeling of granular flow with thermal transfer: application to the discharge of silos, Appl. Therm. Eng. 29 (2009) 1846–1853.